Structural and electronic properties of bulk ZnSe

A. Continenza, S. Massidda, and A. J. Freeman
Department of Physics and Astronomy and Materials Research Center, Northwestern University, Evanston, Illinois 60208
(Received 30 June 1988)

Results of a highly precise all-electron total-energy calculation of the equilibrium lattice constant, bulk modulus, cohesive energy, band structure, pressure dependence of the gap, density of states, and charge density are presented for ZnSe. The calculation is performed within the local-density approximation using the all-electron full-potential linear-augmented-plane-wave (FLAPW) method. The results obtained are compared with other calculations and with the experimental data available for the structural properties and from photoemission spectra measurements; good agreement with these experiments is found. In particular, the study of the direct band gap as a function of the pressure shows that it does not transform into an indirect band gap and, moreover, that the correct behavior is predicted.

I. INTRODUCTION

Technological and theoretical interest in ZnSe has been growing recently due to its appealing electrical and optical properties. Considerable effort is being devoted to realize a *p*-type material by using different techniques as, for example, by doping or growing with impurities such as Li or Cl.[1-3] Further, ZnSe has proved to be a particularly interesting dilute magnetic semiconductor when doped with Mn.[4-6] Finally, the very recent molecular-beam-epitaxy (MBE) growth of bcc Fe and Ni single crystals on ZnSe (Ref. 7) is opening up the possibility of using such materials as microelectronic magnetic switches.

From the theoretical point of view, many authors have studied this semiconductor in order to explore, in more detail, its electronic properties; among the various previous calculations[8-13] of the electronic properties of ZnSe we will particularly refer to the recent work of Bernard and Zunger[12] and Jansen and Sankey.[13] The method used in the last reference is based on a pseudopotential scheme and describes the electronic states as a combination of "pseudo-atomic-orbitals." As the authors affirm, this calculation does not require any experimental input and does not have any adjustable parameters, but, as we will discuss later, it does not consider the Zn 3*d* orbitals as part of the valence states. The calculations performed by Bernard and Zunger[12] are based on a mixed-basis all-electron method which considers a combination of plane waves and localized orbitals which are obtained by solving an atomic problem in which the potential is taken to be equal to the crystal potential. However, the ground-state structural and cohesive properties of this material have not been widely investigated as has been done for other semiconductors (e.g., GaAs or AlAs); apart from the calculations performed in Refs. 13 and 14, to the best of our knowledge, no such other calculations have been reported in the literature.

Here we present results of highly precise self-consistent all-electron total-energy calculations of the ground-state structural, electronic, and cohesive properties of ZnSe, and provide a comparison with previous calculations and the experimental data available in the literature. To this end, we performed an all-electron total-energy band-structure calculation using the self-consistent full-potential linear-augmented-plane-wave band method[15] (FLAPW) within the local-density approximation (LDA).

II. METHOD

The crystal structure of ZnSe is zinc-blende with two atoms per unit cell; the full space group is T_d^2 ($F\bar{4}3m$), which includes 24 symmetry operations and excludes inversion symmetry. In the calculation, 2891 plane waves have been used for the expansion of the charge density and the potential in the interstitial region, and lattice harmonics up to $l=8$ for the expansion inside the muffin-tin spheres. The dependence of the total energy on the number of $\mathbf{k}$ points in the irreducible wedge of the first Brillouin zone (BZ) has been explored within the linearized tetrahedron scheme[16] by performing the calculation for 40 and 60 $\mathbf{k}$ points and extrapolating to an infinite number of $\mathbf{k}$ points. We also used the special $\mathbf{k}$ points technique[17] and the results obtained for the equilibrium properties are compared with those obtained by using the linear tetrahedron method. A satisfactory degree of convergence was achieved by considering a number of FLAPW basis functions up to $R_{\mathrm{MT}}K_{\mathrm{max}}=8.97$ (where R_{MT} is the average radius of the muffin-tin spheres and K_{max} is the maximum value of the wave vector $\mathbf{K}=\mathbf{k}+\mathbf{G}$). This corresponds, at the equilibrium lattice constant, to about 300 basis functions. In order to keep the same degree of convergence for all the lattice constants studied, we kept the values of the sphere radii and of K_{max} constant over all the range of lattice spacings considered.

As exchange-correlation potential, we used the Hedin-Lundqvist[18] form, but we also tried the Ceperley-Alder[19] parametrization in order to see the dependence of the semiconducting gap on the exchange-correlation potential. The semirelativistic approximation (no spin-orbit effects included) was employed in the calculation of the

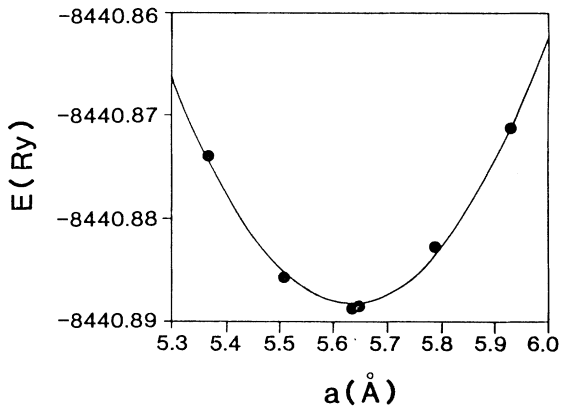

FIG. 1. Total energy E (in Ry) as a function of the lattice spacing a (in Å), calculated with the special-**k**-points technique (Ref. 17).

valence-band states, whereas the core levels were treated fully relativistically and were self-consistently updated at each iteration. The $3d$ electrons of the Zn atom were treated as part of the valence band since they are relatively high in energy even though they constitute a well-localized and narrow band. This makes the calculation easier to converge, even though we need quite a large value for the product $K_{\max}R_{\mathrm{MT}}$ in order to have a suitable number of plane waves to correctly describe these states.

III. RESULTS

A. Structural properties

Figure 1 shows a plot of the total energy as a function of the lattice constant calculated using ten special **k** points.[17] In Table I we report the bulk properties as obtained using these 10 special **k** points as well as 40 and 60 **k** points in the irreducible Brillouin-zone (BZ) wedge with the linear tetrahedron method. We then extrapolate up to an infinite number of **k** points, knowing that the error in the total energy decreases as $(n_k)^{-2/3}$ where $n_{\mathbf{k}}$ is the number **k** points used.[20]

The cohesive energy was computed from the difference between the total atomic energies, calculated for the ground-state configurations of Zn($4s^2$) and Se($4s^24p^4$) including spin polarization, and the minimum energy of bulk ZnSe calculated at the equilibrium lattice constant (a_0). The bulk modulus is obtained from the curvature of the total energy as a function of the lattice constant [$B=(4/9a_0)d^2E/da^2$] and has been determined by fitting the calculated energy values with a parabola. The equilibrium lattice constant obtained from the minimum of the parabola which best fits the calculated results in Fig. 1 is very close to the experimental value, with only a 0.6% deviation obtained with the special-**k**-points method. As expected, the calculated bulk modulus and cohesive energy show a larger deviation from the observed values,[21,22] but the discrepancy in the case of the bulk modulus is smaller than that obtained in another LDA calculation (Refs. 13 and 23) or with Cohen's empirical method (Ref. 14). As far as the cohesive energy is concerned, the calculated value overestimates the experimental one, showing a quite large deviation. Although a comparison with other LDA calculations is not possible because of the lack of published data, we believe that the deviation from the experimental value is mainly due to the LDA which is known to underestimate,[15] in the atomic calculations, the contribution to the total energy coming from the outermost atomic shells whose electronic charge density is not homogeneously distributed in the regions around the nucleus.

The calculated results reported in Table I show that the special-**k**-points technique is particularly suitable in the case of semiconductors and gives very good results. The larger discrepancies found by the linear tetrahedron method are probably due to the fact that a relatively small number of **k** points (up to 60) was used to extrapolate to an infinite number of **k** points. This also shows that the linear tetrahedron scheme requires a larger number of **k** points to get good accuracy, even in the simple case of semiconductors, in order to minimize the errors associated with the use of a linear interpolation on a limited set of **k** points.

B. Band structure and density of states

The band structure, calculated at the equilibrium lattice constant given in Fig. 1, is shown in Fig. 2. The

TABLE I. Bulk properties: results obtained in the present calculation and other theoretical results compared (as a percentage deviation) with experimental data.

	a (Å)	Δ (%)	B (Mbar)	Δ (%)	E_{coh} (eV)	Δ (%)
10 **k** points	5.6357	0.6	0.667	6.7	5.57	27
40 **k** points	5.6202	0.8	0.688	10.0	5.71	30
60 **k** points	5.6173	0.9	0.678	8.5	5.72	31
∞ **k** points	5.6067	1.0	0.639	2.2	5.76	31
Ref. 13	5.5	>2	0.76	>10		
Ref. 14			0.75	17.2		
Ref. 23		0.2	0.602	3.8		
Expt.	5.6676[a]		0.625[b]		4.38[a]	

[a]Reference 21.
[b]Reference 22.

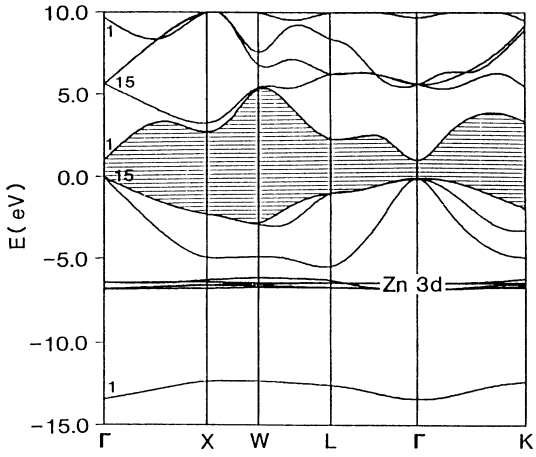

FIG. 2. Calculated self-consistent band structure of ZnSe.

main features agree closely with the results obtained previously.[12,13] In the following, we will discuss the band structure together with the total and partial density of states (DOS and PDOS) per atom, shown in Fig. 3, in order to better identify the origin and the character of each feature. For simplicity, the zero energy in Figs. 2 and 3 is considered to coincide with the top of the valence band (Γ_{15v}). The energy region shown at low energies includes the peaks due to the Se 4*s* (Γ_1) and the Zn 3*d* states; these states are, in fact, well localized at about -13 and -6.5 eV, respectively, from the top of the valence band [Se *p* states (Γ_{15v})] with a width of about 2.0 and 1.0 eV, respectively.

The two peaks below the Fermi level correspond to the Se 4*p* levels partially mixed with the Zn 4*s* and 3*d*; the features above the Fermi level originate mainly from the 4*s* and 4*p* states of Zn partially hybridized with the Se states. By looking in more detail at the main valence band, we found that the corresponding DOS has a well-defined structure. In particular, the levels mostly due to

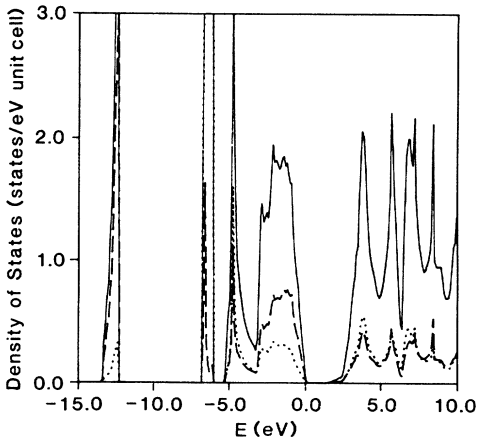

FIG. 3. Total and partial density of states (DOS) per atom (the dashed line represents the Se contribution, the dotted line represents the Zn contribution).

the bonding of the cation 4*s* and 4*d* with the anion 4*p* orbitals form a sharp and well-defined peak in the DOS at about -5 eV. The broader peak just below the Fermi level originates mainly from the hybridization of the anion 4*p* with the cation 4*d* and 4*p* levels. Remarkably, the contribution due to the outermost cation *d* levels adds up to about 18% of the total contribution, stressing the importance of the role played by these levels in determining the character and the structure of the valence band of the compound. In this regard, our all-electron calculation agrees with the results of Bachelet and Christensen[24] for GaAs, Christensen,[25] and Bernard and Zunger[12] regarding the importance of correctly considering such states in a band-structure calculation in order to properly describe the properties of the material. Actually, as has been noticed previously, in the case of semiconductors having *d* orbitals in the valence band (as in the ZnSe case), there is a repulsion coming from symmetry effects that must be accounted for.[12] In fact, the Zn *d* as well as the Se *p* orbitals have a component which transforms according to the Γ_{15} representation; the bonding-antibonding interaction that arises between these symmetrically similar levels then repels the top of the valence band (i.e., Se 4*p*) causing an overall reduction of the direct gap.

C. Pressure dependence of the energy gaps

In Table II, we report values of the direct (E_g^Γ) and indirect (E_g^X,E_g^L) gaps calculated as a function of pressure. Compared with the experimental value of the gap at the equilibrium lattice spacing[21] [$(E_g^\Gamma)_{\text{expt}}=2.80$ eV], the calculated value is very small; this is, however, not too surprising if one recalls, as is well known, that the LDA underestimates the energy gap in the case of insulators and semiconductors since it does not give a proper description of the excitation properties of the system.

In agreement with experiment,[23] the direct band gap increases with pressure and does not transform into an indirect band gap, as observed in other semiconductors (GaAs, GaP, and InP). In the ZnSe case, in fact, the calculated indirect band gaps (E_g^X and E_g^L) are much larger (by ~ 1 eV) than E_g^Γ for a wide range of pressure, and this is also in agreement with the experimental observations. In order to compare with the experimental data, we fitted our results with a second-order polynomial expansion following the method described in Ref. 23, and also con-

TABLE II. Dependence of the direct and indirect band gaps on lattice constant for positive and negative pressures.

a (Å)	E_g^Γ (eV)	E_g^X (eV)	E_g^L (eV)	$\Delta a/a_0$ (%)
5.3675	1.73	2.44	2.64	−4.8
5.5088	1.39	2.64	2.50	−2.3
5.6357	1.10	2.79	2.38	0.0
5.6500	1.07	2.81	2.32	0.25
5.7913	0.78	2.96	2.24	2.76
5.9325	0.52	3.09	2.10	5.27

TABLE III. Experimental and calculated parameters of direct band gap vs lattice constant as fitted to Eq. (1). All values are given in eV.

	E_g^Γ (a_0)	b	c
Expt.[a]	2.685	14.4±0.4	6.2±0.4
Present calc.	1.10	12.1	21.2
Pseudopotential[a]	2.695	14.9	−125.7
LMTO-ASA[a]	1.16	12.95	−26.8

[a]Reference 23.

sidered the negative pressure region,

$$E_g^\Gamma(a)=E_g^\Gamma(a_0)+b\left[-\frac{\Delta a}{a_0}\right]+c\left[-\frac{\Delta a}{a_0}\right]2\ . \qquad (1)$$

The values of the coefficients obtained from this fitting are shown in Table III, along with other calculations and experimental values for comparison. We should point out that the range of pressure ($\Delta a/a_0$) we considered is quite limited and that, as stated, we also included in the fitting the region of negative pressure; if that region is excluded, we obtained, for a pure linear fitting, $b=13.1$ eV. The results of our calculation compare satisfactorily with the experiments and give, especially for the c coefficient, a value much closer to the experimental result than do other calculations.[23]

Remarkably, our calculation predicts the correct curvature (the sign of the c coefficient) recovering the slight supralinearity dependence of E_g^Γ as a function of ($\Delta a/a_0$) observed by the experiments.[23] Our result is therefore proof that the deviations between the theoretical results and experiment presented in Ref. 23 are not to be attributed to errors introduced by the LDA, as might be suggested.[23] The reasons for such deviations are to be sought, instead, in the role played by the Zn 3d electrons: Our calculation seems, in fact, to confirm the hypothesis[23] that the nonsphericity of the charge density due to such states is an important factor to take into account in order to correctly describe the behavior of the direct gap under pressure.

D. Comparison with photoemission and other calculations

Table IV presents the energy levels referred to the top of the valence band at selected symmetry **k** points for the calculated equilibrium lattice spacing, compared with photoemission experimental data.[26–28] Note that the agreement is rather good for the valence states, except for the 3d [$\Gamma_{15v}(d),\Gamma_{12v}(d)$] levels of the cation (listed only for the Γ point) and the 4s band of the anion, which are lower in the experiment, by about 2.6 and 1.8 eV, respectively. It is now generally accepted that this discrepancy is certainly due to correlation and relaxation effects which arise in the ionization of a core level and are underestimated in a local-density calculation. In particular, one should note that the discrepancy regarding the Zn 3d levels has been shown[29] to be removed by including self-interaction-correction terms. In addition, the precise determination of the anion s-level position is quite hard to obtain experimentally due to the large superimposed secondary-emission background.

Table V lists the energy levels at Γ, X, L, referred to the top of the valence band together with the results obtained in previous calculations for somewhat different lattice constants. Given the small deviation among the various lattice spacings used ($<0.7\%$), this should not, however, affect dramatically the comparison; we expect that the difference would be of the order of 0.01–0.05 eV depending on the symmetry point and on the nature of the energy eigenvalue. Very good agreement is found with the results of the energy eigenvalue. Very good agreement is found with the results of similar FLAPW calculations by Hamada,[30] which used the Ceperley-Alder exchange-correlation functional. The value of the band gap is remarkably close, as is the position of most of the other energy levels. The main discrepancy, found for the Zn 3d levels, might be due to the different computational details involved in carrying out the two calculations.

Our results compare quite well, also, with those of Bernard and Zunger,[12] and to a lesser extent with those of Jansen and Sankey[13]—the main difference being the position of the Se 4s bands which are deeper, in our case, by about 0.5 eV, and the Zn 3d, which are higher by about

TABLE IV. Energy levels (eV) at high-symmetry **k** points compared with photoemission spectra.

Point Γ			Point X			Point L		
	Calc.	Expt.		Calc.	Expt.		Calc.	Expt.
Γ_1	−13.43	−15.2±0.6[a]	X_1	−12.33	−12.5±0.4[a]	L_1	−12.61	−13.1±0.3[a]
$\Gamma_{15v}(d)$	−6.79	−9.2±0.15[a]	X_{3v}	−4.92	−5.3±0.3[b]	L_{3v}	−0.91	−1.3±0.3[a]
		−8.9±0.4[c]						0.7±0.2[b]
$\Gamma_{12v}(d)$	−6.42	−8.6[b]	X_{5v}	−2.27	−2.1±0.3[a]			
Γ_{15v}	0.00	0.0[a]						
Γ_{1c}	1.10	2.80[a]	X_{1c}	2.73		L_{1c}	2.38	
Γ_{15c}	5.69		X_{3c}	3.33		L_{3c}	6.32	
Γ_{1c}	9.70							

[a]Reference 26.
[b]Reference 27.
[c]Reference 28.

TABLE V. Calculated energy eigenvalues (in eV) at high-symmetry points in the BZ as obtained in the present calculation ($a_o = 5.6357$ Å) using the Hedin-Lundqvist (HL) and Ceperley-Alder (CA) exchange-correlation potentials, compared with those of other calculations. Note: The results in Ref. 12, 13, and 30 refer to the experimental lattice constant ($a_0 = 5.668$ Å) and have been obtained with the Ceperley-Alder exchange-correlation potential; those of Ref. 8 are for $a_0 = 5.65$ Å and use the Slater ($\alpha = 1$) exchange approximation.

	Present Calc. (HL)	Present Calc. (CA)	Ref. 30	Ref. 12	Ref. 13	Ref. 8
Γ_1	−13.43	−13.37	−13.25	−12.86	−12.54	−11.82
$\Gamma_{15v}(d)$	−6.79	−6.77	−7.64	−7.86		−12.6
$\Gamma_{12v}(d)$	−6.42	−6.41	−7.20	−7.60		
Γ_{15v}	0.0	0.0	0.0	0.0	0.0	0.0
Γ_{1c}	1.10	1.08	1.07	1.45	2.07	2.94
Γ_{15}	5.69	5.70	5.82	5.77	5.87	6.66
Γ_1	9.70	9.69	9.75	9.79		
X_1	−12.33	−12.30	−12.12	−11.79	−11.12	−10.48
X_{3v}	−4.92	−4.89	−4.91	−4.82	−4.75	−4.31
X_{5v}	−2.27	−2.24	−2.10	−2.20	−2.12	−1.65
X_{1c}	2.79	2.82	2.98	2.88	3.16	4.19
X_{3c}	3.33	3.34	3.38	3.47	3.75	4.49
X_{1c}	10.64	10.59	10.67	10.58		
L_1	−12.61	−12.57	−12.43	−12.06	−11.48	−10.84
L_{1v}	−5.41	−5.35	−5.16	−5.21	−4.99	−4.40
L_{3v}	−0.31	−0.91	−0.85	−0.87	−0.85	−0.64
L_{1c}	2.38	2.37	2.40	2.63	3.04	3.79
L_{3c}	6.32	6.33	6.46	6.36	6.57	7.31
L_{1c}	8.43	8.42				

1.0 eV with respect to Ref. 12. Better agreement is found, for these states, with the linear muffin-tin-orbital (LMTO) calculations reported by Ves *et al.*[23] (−6.7 eV). Besides these states, larger discrepancies are observed in the direct band gap, which is smaller in our case (by ~0.3 and ~1.0 eV compared with those of Bernard and Zunger[12] and Jansen and Sankey,[13] respectively). It must be noticed that the discrepancy with the result of Ref. 13 regarding the gap value is mainly due to the fact that this calculation does not include the Zn 3*d* levels as part of the valence states. It, therefore, neglects the Zn 3*d* relaxation and the effect of the repulsion on the valence-band top; it overestimates as a result, the band-gap value.

We must further point out that the results of Refs. 12, 13, 30, and 8 were all obtained with different exchange-correlation functionals: in particular, in Ref. 8 the Wigner form was used, whereas in Refs. 12, 13, and 30 the Ceperley-Alder parametrization was considered. In order to see how the parametrized form of the exchange-correlation affects the position of the energy levels and the gap itself, we performed a calculation using the Ceperley and Alder exchange-correlation functional as parametrized by Perdew and Zunger.[19] The results are shown in Table V for comparison; we found that the energy values were only slightly affected (by ≤ 0.05 eV). Hence, the reasons for the discrepancy with the results of Refs. 12 and 13 must be sought in the different methods used.

TABLE VI. Decomposition of charge into different angular-momentum contributions inside the muffin-tin spheres. The muffin-tin sphere radii are $R_{MT} = 2.09$ a.u. for Se and $R_{MT} = 2.3$ a.u. for Zn.

	Q_s	Q_p	Q_d	Q_{MT}
Se	1.365	2.223	0.026	3.619
Zn	0.539	0.453	9.758	10.768

E. Bonding and ionic character

In Table VI, we show the total integrated charge per atom decomposed into different angular-momentum contributions; note that the quantities shown, Q_l, correspond to the total charge inside each muffin-tin sphere, and that

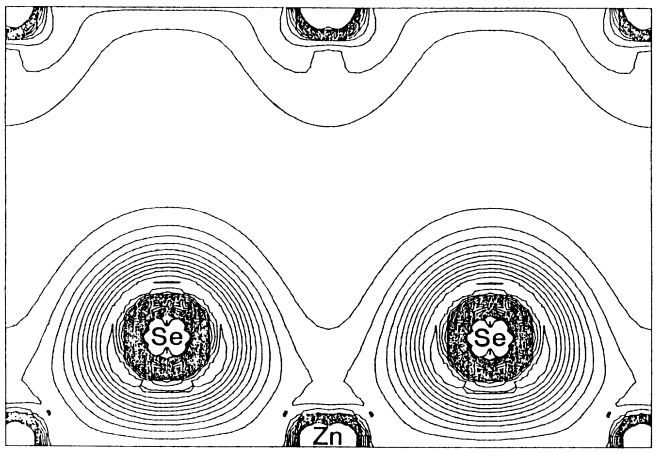

FIG. 4. Valence charge density at the equilibrium lattice constant in the (110) plane; values are in 1×10^{-2} e/(a.u.)^3.

even though we used different sphere radius values for Se and Zn, the use of the full-potential feature ensures that the calculation is completely independent of the choice of the sphere radii.

The ionic character of the Zn—Se bond is not very transparent from the total charge contained in the muffin-tin spheres as shown in Table VI due to the large difference between the radii values used. For this reason we show in Fig. 4 the self-consistent valence charge density in the (110) plane as obtained by subtracting out the contribution of the Zn 3*d* levels in order to demonstrate the Zn—Se bonding charge density. The highly spherical shape of the charge surrounding the Se atom suggests, together with the lack of an important bonding charge between Zn and Se, that a large part of the Zn 4*s* electrons is almost completely transferred to the Se site. This can also be inferred from the results shown in Table VI, noticing that inside the Zn sphere there are only 0.54 *s*-like electrons, even though the Zn-sphere radius is 10% larger than that for Se.

ACKNOWLEDGMENTS

We are very grateful to Dr. N. Hamada for helpful discussions and for sharing his results with us before publication. This work was supported by the National Science Foundation (Grant No. DMR-85-20280 through the Northwestern University Materials Research Center), and by a computing grant from its Division of Advanced Scientific Computing at the National Center for Supercomputing Applications, University of Illinois at Urbana-Champaign (Urbana, IL).

[1]T. Yasuda, I. Mitsuischi, and H. Kukimoto, Appl. Phys. Lett. **52**, 57 (1988).
[2]H. Cheng, J. M. DePuydt, J. E. Potts, and T. L. Smith, Appl. Phys. Lett. **52**, 147 (1988).
[3]K. Ohkawa, T. Mitsuyu, and O. Yamazaki, J. Appl. Phys. **62**, 3216 (1987).
[4]S. K. Chang, D. Lee, H. Nakata, A. V. Nurmikko, L. A. Kolodziejski, and R. L. Gunshor, J. Appl. Phys. **62**, 4835 (1987).
[5]J. K. Furdyna, J. Appl. Phys. **53**, 7637 (1982).
[6]Q. Fu, A. V. Nurmikko, L. A. Kolodziejski, R. L. Gunshor, and J. W. Wu, Appl. Phys. Lett. **51**, 578 (1987).
[7]G. A. Prinz, B. T. Jonker, J. J. Krebs, J. M. Ferrari, and F. Kovanic, Appl. Phys. Lett. **48**, 1756 (1986); G. A. Prinz, B. T. Jonker, and J. J. Krebs, Bull. Am. Phys. Soc. **33**, 562 (1988).
[8]D. J. Stukel, R. N. Euwema, T. C. Collins, F. Herman, and R. L. Kortum, Phys. Rev. **179**, 740 (1969).
[9]J. R. Chelikowsky, D. J. Chadi, and M. L. Cohen, Phys. Rev. B **8**, 2786 (1973).
[10]J. R. Chelikowsky and M. L. Cohen, Phys. Rev. B **14**, 556 (1976).
[11]C. S. Wang and B. M. Klein, Phys. Rev. B **24**, 3393 (1981).
[12]J. E. Bernard and A. Zunger, Phys. Rev. B **36**, 3199 (1987).
[13]R. W. Jansen and O. F. Sankey, Phys. Rev. B **36**, 6520 (1987).
[14]M. L. Cohen, Phys. Rev. B **32**, 7988 (1985).
[15]H. J. F. Jansen and A. J. Freeman, Phys. Rev. B **30**, 561 (1984).
[16]J. Rath and A. J. Freeman, Phys. Rev. B **11**, 2109 (1975); O. Jepsen and O. K. Andersen, Solid State Commun. **9**, 1763 (1971); G. Lehman and M. Taut, Phys. Status Solidi **54**, 469 (1972).
[17]A. Baldereschi, Phys. Rev. B **7**, 5212 (1973); D. J. Chadi and M. L. Cohen, Phys. Rev. B **8**, 5747 (1973).
[18]L. Hedin and B. I. Lundqvist, J. Phys. C **4**, 2064 (1971).
[19]J. P. Perdew and A. Zunger, Phys. Rev. B **23**, 5048 (1981).
[20]B. I. Min, H. J. F. Jansen, and A. J. Freeman, Phys. Rev. B **33**, 6383 (1986).
[21]*American Institute of Physics Handbook* (McGraw-Hill, New York, 1987), Table I, p. E-102.
[22]B. H. Lee, J. Appl. Phys. **41**, 2982 (1970).
[23]S. Ves, K. Strössner, N. E. Christensen, C. K. Kim, and M. Cardona, Solid State Commun. **56**, 479 (1985).
[24]G. B. Bachelet and N. E. Christensen, Phys. Rev. B **31**, 879 (1985).
[25]N. E. Christensen, Phys. Rev. B **37**, 4528 (1988).
[26]L. Ley, R. A. Pollak, F. R. McFeely, S. P. Kowalczyk, and D. A. Shirley, Phys. Rev. B. **9**, 600 (1974).
[27]D. E. Eastman, W. D. Grobman, J. L. Freeouf, and M. Erbudak, Phys. Rev. B **9**, 3473 (1974).
[28]C. J. Veseley, R. C. Hengehold, and D. W. Langer, Phys. Rev. B **5**, 2296 (1972).
[29]M. R. Norman, Phys. Rev. B **29**, 2956 (1984).
[30]N. Hamada (private communication).